

Article

Mechanical Properties of Buried Gas Pipeline under Traffic Loads

Jiaxin Zhang ^{1,2}, Xiaoting Gu ^{1,2,*}, Yutong Zhou ³, Yu Wang ⁴, Hailun Zhang ^{1,2} and Yuan Zhang ⁵¹ College of Petroleum Engineering, Yangtze University, Wuhan 430100, China; 1507113712@163.com (J.Z.)² Hubei Key Laboratory of Oil and Gas Drilling Engineering, Yangtze University, Wuhan 430100, China³ National Pipeline Network Group Eastern Crude Oil Storage and Transportation Co., Ltd., Xuzhou 220005, China⁴ College of Storage, Transportation and Construction Engineering, China University of Petroleum (East China), Qingdao 266580, China⁵ Production Command Center, Qinghai Oilfield Underground Operation Company, Mangya 816499, China

* Correspondence: xiaotinggu@yangtzeu.edu.cn

Abstract: Dynamic loads generated by heavy vehicles are among the loads resisted by pipelines buried under road surfaces. Most recent analyses are based on static assumptions; however, in practice, vehicle loads change dynamically. In this study, the finite element model of the pipe–soil interaction of a buried pipeline was established using the ABAQUS 2020 finite element software, and dynamic loads were applied above the model soil to simulate the influence of vehicles above the highway on the buried X80 pipeline. The mechanical responses of different influencing factors to buried pipelines were analyzed. Increasing the pipe diameter and burial depth decreases the effect of vehicle rolling on the buried pipeline. The mass of the vehicle is the most significant factor that influences the stress and strain on the pipeline. The stress increase of the conventional vehicle load on the X80 gas pipeline does not exceed 10 MPa, and the maximum shape variable of the pipeline is within 13 mm. This study provides a data reference and a risk warning regarding the rolling of buried natural gas pipelines under a single vehicle load.

Keywords: buried pipelines; traffic loads; finite elements; X80



Citation: Zhang, J.; Gu, X.; Zhou, Y.; Wang, Y.; Zhang, H.; Zhang, Y. Mechanical Properties of Buried Gas Pipeline under Traffic Loads. *Processes* **2023**, *11*, 3087. <https://doi.org/10.3390/pr11113087>

Academic Editors: Fadl A. Essa and Bahaa Saleh

Received: 22 September 2023

Revised: 17 October 2023

Accepted: 24 October 2023

Published: 27 October 2023



Copyright: © 2023 by the authors. Licensee MDPI, Basel, Switzerland. This article is an open access article distributed under the terms and conditions of the Creative Commons Attribution (CC BY) license (<https://creativecommons.org/licenses/by/4.0/>).

1. Introduction

In recent years, accidents involving pipeline damage, leaks, and fires caused by vehicles running over pipelines have frequently occurred. In 2018, a bus in Beibei District, Chongqing, ran over a gas pipeline while in motion, which resulted in gas leaks and subsequent fires. In 2020, a concrete tanker truck in Xiuwu County, Henan Province, ran over an oil pipeline while being driven, which led to oil leaks and explosions. In 2021, a similar incident occurred in the Wuhan area, involving a gas leak with clear evidence of vehicle impact marks [1]. The impact of heavy vehicles running over pipelines significantly compromises safety. When pipelines bear loads from vehicles, the loads can lead to pipeline damage, potentially causing accidents such as leaks and explosions. These incidents can cause significant damage to property and threaten the lives of nearby residents. Therefore, assessing pipeline stress conditions and ensuring pipeline safety are vital.

Specifications related to pipeline safety are “GB 50423-2013 Code for Design of Oil and Gas Transportation Pipeline Crossing Engineering”, “API 1160 Managing System Integrity for Hazardous Liquid Pipelines”, “B31.8S-Managing System Integrity of Gas Pipelines”, and “PD 8010-4:2012 Pipeline Systems Steel Pipelines on Land and Subsea Pipelines.” Code of Practice for Integrity Management” et al. And researchers have extensively investigated the mechanical performance of buried gas pipelines under traffic loads. Phillips et al. [2] established a three-dimensional finite element parametric model to simulate and analyze the interaction between pipes and soil under combined axial and lateral loads.

Yimsiri et al. [3] investigated the influence of lateral and longitudinal movements of a foundation on pipe–soil interactions under deeply buried conditions. Alzabeebee [4] compared the responses of buried pipelines to static and dynamic loads using finite element numerical simulations. Anirban C. Mitra [5] used a quarter-car model. The influence of suspended and non-suspended mass distribution, tire pressure, vehicle speed, leaf spring, and damper stiffness on the dynamic load coefficient of the vehicle was preliminary analyzed in Adams/Car. Li B [6] innovatively developed a system for testing the integrity of buried pipelines under traffic loads, internal corrosion, and corrosion cavities and established a multi-parameter formula through parametric analysis that can accurately predict the maximum stress of pipelines with corrosion voids and internal corrosion. Rakitin B [7] presented geotechnical centrifuge tests on a large reinforced concrete pipe under heavy traffic loads, revealing the significant impact of soil cover depth and traffic load positions on pipe bending moments, with unconservative results noted for shallow soil cover depths and heavy traffic loads when compared to conventional design methods. Zamanian S. [8] employed global sensitivity analysis to assess the impact of corrosion and traffic loads on the service life of sewer pipes, revealing that concrete strength, environmental factors, and truck-related variables are the most influential sources of uncertainty over time. Robert D. J. [9] investigated the performance monitoring of field-buried water pipes using comprehensive field instrumentation, revealing varying strains under traffic loads and internal water pressure and providing valuable data to enhance the prediction and maintenance of aging water pipelines. Wu [10] employed the ABAQUS software to simulate and compute the stress characteristics of pipelines in soft soil foundations under traffic loads. Wang [11] combined theoretical analysis, numerical simulations, and case studies to assess static analysis, dynamic response, and load-reduction measures for buried pipelines. Liao [12] used the ABAQUS finite element software to investigate the stress-strain behavior of buried natural gas pipelines under various conditions. Zhang [1] examined the effects of factors such as heavy vehicle mass, pipe diameter, wall thickness, and internal pressure on the axial mechanical response of pipelines.

Research on the dynamic loads induced by vehicular movement in high-strength buried gas pipelines is predominantly based on static assumptions. Previous studies have often divided the entire dynamic process into multiple static phases, determined the wheel loads of vehicles at different positions, frequencies, and magnitudes, and converted them into equivalent static loads on the pipeline. Although static models typically approximate dynamic loads in most scenarios, a more detailed analysis is required in special cases, such as sudden transient loads, for example, earthquakes, explosions, and cyclic vibration loads, to ensure safety and reliability. Therefore, by using ABAQUS and employing the VDLOAD subroutine to simulate the load outputs as dynamic loads, this study investigated the stress and strain in buried gas pipelines under various conditions. The effects of parameters such as pipeline diameter, burial depth, vehicle loads, and the internal pressure of the medium on the mechanical performance of gas pipelines were investigated. This study provides a theoretical foundation for designing and constructing buried pipelines.

2. Finite Element Model

A VDLOAD subroutine was developed to account for the mobility of vehicle-induced moving loads and analyze the pressure distribution between the road surface and wheels. This subroutine defines the output parameters, encompassing the geometric characteristics of the road surface and wheels as well as the load conditions. Based on the user-provided parameters, it computes the magnitude and distribution of the contact forces between the road surface and wheels. The computed results are integrated into ABAQUS as input loads to analyze the stress and strain of the structures. The contact area between a single wheel of the vehicle and the soil was $0.3 \text{ m} \times 0.24 \text{ m}$. The VDLOAD subroutine facilitates the dynamic load input [13]. Dynamic implicit simulations were conducted using ABAQUS, with an overall runtime of 0.6 s and a vehicle speed of 15 m/s, to assess the mechanical behavior of the entire vehicle passing over the pipeline.

2.1. Pipeline Parameters

X80-grade steel was used in this study. The material had a pipe density of 7800 kg/m³, an elastic modulus of 210 GPa, and a Poisson's ratio of 0.3 [14]. The selected approach for pipeline analysis involved using the Ramberg–Osgood constitutive equation to describe the stress–strain behavior of the pipe material, as represented by the stress–strain relationship [15,16]. This is represented by Equation (1):

$$\varepsilon = \frac{\sigma_0}{E} \left[1 + \frac{\alpha}{1 + \nu} \left(\frac{\sigma_0}{\sigma_s} \right)^\nu \right] \quad (1)$$

where ε is the true strain, E is the elastic modulus (GPa), σ_s is the yield strength of the pipe material (MPa), σ_0 is the uniaxial tensile stress (MPa), α is the hardening coefficient, and ν is the power hardening exponent.

The stress–strain curve of X80 steel is shown in Figure 1.

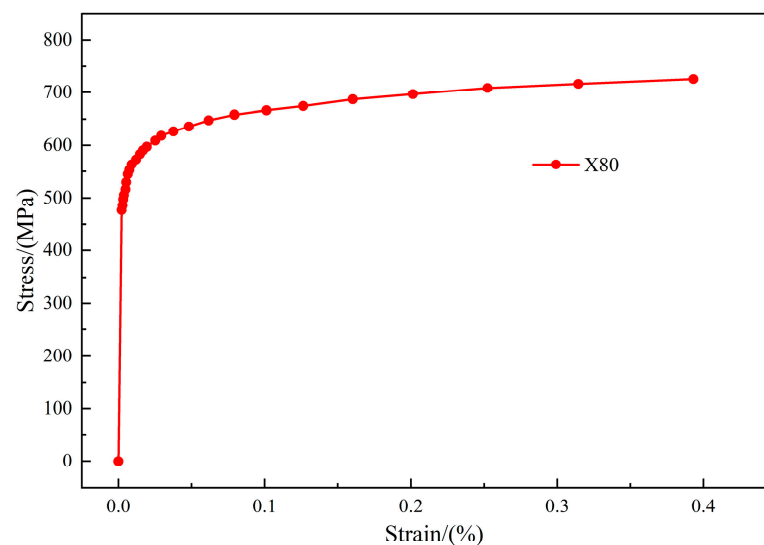


Figure 1. Stress–strain curve of X80 steel.

Given that the wall thickness of a pipeline is relatively thin, typically much smaller than the overall dimensions of the structure (approximately one-tenth of its thickness), adopting a shell-element structure facilitates a more accurate simulation of the deformation and stress distribution of the pipeline under loads. Shell-element structures exhibit excellent applicability and accuracy when considering the stress conditions of thin-walled structures.

2.2. Soil Parameters

The soil was simplified using a linearly elastic model because of its simplicity and versatility, which facilitate its integration with other models. The Drucker–Prager model [17] was employed for the soil; the parameters are listed in Table 1.

Table 1. Soil parameters.

Density (kg/m ³)	Young's Modulus (MPa)	Poisson's Ratio	Angle of Friction (°)	Flow Stress Ratio	Expansion Angle (°)
1780	14.4	0.4	36	1	0

During vehicle operations, the impact on the sides of the road is minimal, and the mechanical response can be almost negligible. This is because the influence of vehicles is primarily concentrated in the central region of the road. In the direction of vehicle motion, the effect of the vehicle on the far distance is virtually nonexistent. The thickness of the

underlying soil base of the road is assumed to be infinitely large and has a negligible impact on the mechanical response of the road surface [18]. Consequently, the soil model was constrained with four lateral displacement boundary conditions, oriented perpendicular to the surfaces, to restrict the displacement in that direction. The bottom boundary conditions were set as fully fixed constraints to maintain the stability of the soil model. Moreover, a Y-direction displacement load was applied to the wheel contact surface to simulate the effect of the vehicle on the road surface [19].

2.3. Pipe–Soil Model

The finite element model considers applied loads, such as the pressure from the wheels to the ground, the internal pipeline pressure, and the self-weight of the soil and pipe. The contact relationship between the pipeline surface and the soil surface was considered to precisely simulate the interaction between the buried pipeline and the soil. In the model, the external surface of the buried pipeline was designated as the master surface, whereas the internal surface of the soil was identified as the slave surface. The contact relationship between the pipe and soil was defined as a surface-to-surface interaction. In the normal direction of the contact surface, a “hard contact” approach was employed, assuming that no gap existed between the pipeline and soil surfaces and allowing for direct normal contact pressure. In the tangential direction of the contact surface, a “penalty function” method was used with a friction coefficient of 0.3 to consider the frictional interaction between the pipe and soil.

For buried natural-gas pipelines, the vehicle load can be approximated as a distributed surface load. The distributed load resembles the actual contact path of a tire with the ground and is widely used in three-dimensional shallow-buried pipeline analysis models [20], which is suitable for this study. The pressure exerted by the vehicle on the road surface is simplified as the pressure from the tire on the contact area with the road surface and is assumed to be uniformly distributed [21]. Numerous studies have shown that the contact shape of a tire resembles a rectangle. The actual contact area between the tire and ground can be approximated as a rectangular area with a tire width of 0.24 m and a contact area length of 0.3 m. This rectangular region represents the contact area between a single tire or a set of rear tires and the ground, with a ground pressure of 0.85 MPa.

Based on the analyses conducted using the pipeline, foundation, and pipe–soil interaction models described above, a specific approach has been adopted for buried gas pipelines that traverse roadways. This approach considers the effects of the pipe self-weight, soil pressure on the upper part of the pipeline, the internal pressure of the transported medium, and traffic loads on the buried pipeline. Consequently, the boundary conditions for the foundation–pipeline system were established. The loading model is shown in Figure 2.

2.4. Failure Criteria

When subjected to traffic loads, pipelines experience a certain level of complexity, resulting in both axial and hoop stresses within the pipeline. In the case of large-diameter, long-distance pipelines, failure occurs when the equivalent stress in the pipeline reaches its yield strength. Typically, the Von Mises equivalent stress calculation, which is based on the Fourth Strength Theory, is employed to assess the pipeline’s performance under these conditions. This is represented by Equation (2):

$$\sigma_{Mises} = \frac{1}{\sqrt{2}} \sqrt{(\sigma_1 - \sigma_2)^2 + (\sigma_1 - \sigma_3)^2 + (\sigma_2 - \sigma_3)^2} = \sigma_s \quad (2)$$

where σ_1 , σ_2 , σ_3 are the first, second, and third principal stresses, respectively, σ_s is the pipe yield stress.

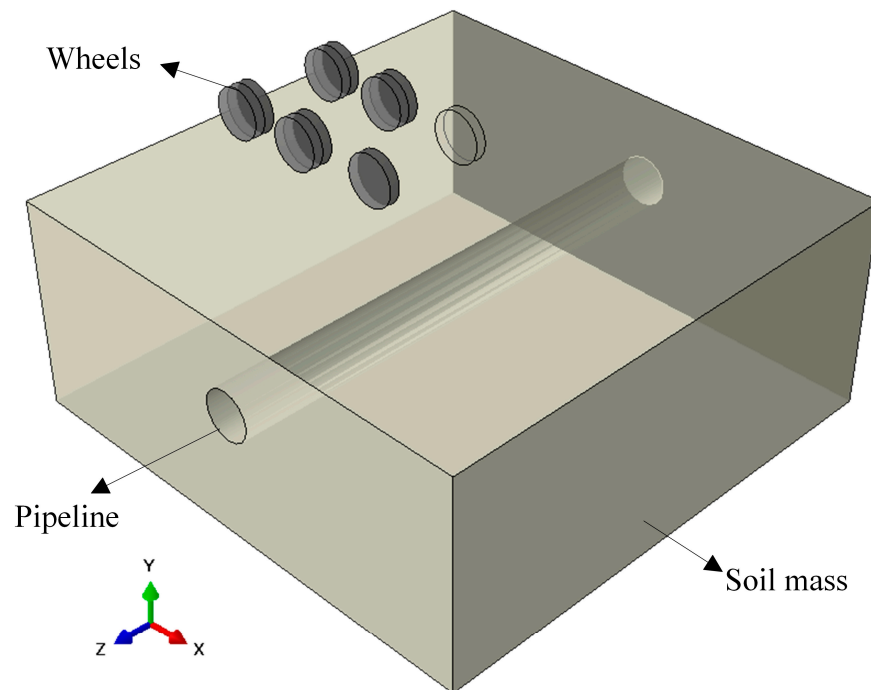


Figure 2. A model diagram of the road surface above the vehicle contact pipe.

3. Model Validation

Based on the proposed model, a finite element simulation approach was used to analyze the axial stress on top of the pipeline when subjected to heavy vehicles overhead. The axial stress distributed along the pipeline was obtained via simulations, as depicted in Figure 3. By employing the same pipeline and soil data, the simulated results showed a maximum difference of 9.67% and a minimum error of 0.36% compared with the data in [21], resulting in an overall error within 10%. The variation in the axial stress along the pipeline was recorded at the moment of peak circumferential stress, with the highest axial stresses constrained at both ends of the pipeline and the lowest points corresponding to positions directly beneath the wheels.

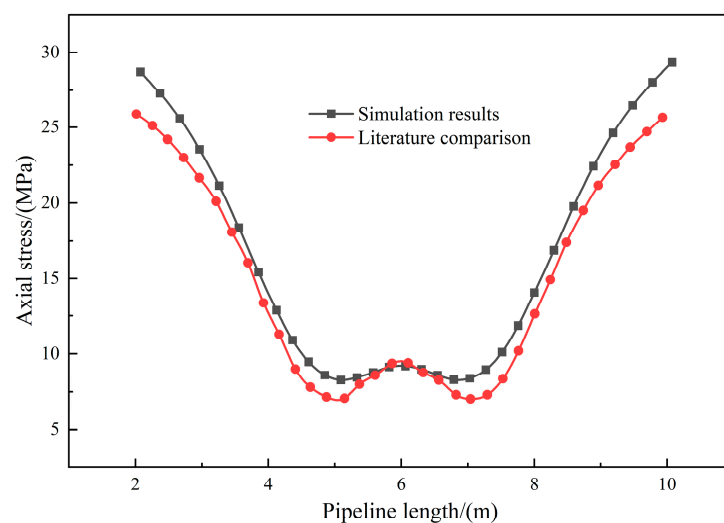


Figure 3. Model validation.

In this study, the mesh division employed a standard element library, utilizing a linear geometric order with C3D8R elements to ensure computational accuracy. The C3D8R

elements, with eight nodes, improved precision while maintaining computational efficiency. Localized mesh refinement was applied to the pipeline area and the region under vehicle pressure to further improve the model accuracy. This refinement allowed for a more detailed representation of the local geometry and physical characteristics. In areas far from the pipeline, a larger mesh was used to balance the computational accuracy and time cost. Because the interaction between the pipeline and soil underwent significant plastic strain during the wheel-rolling process, local refinement was applied to the soil and wheel contact regions. The entire pipe–soil model consisted of 219,688 elements. The resulting finite element model of the pipe–soil system under vehicle pressure is shown in Figure 4. This localized mesh refinement approach captures crucial features of the pipe–soil interaction more accurately, improving the credibility and predictive precision of the model.

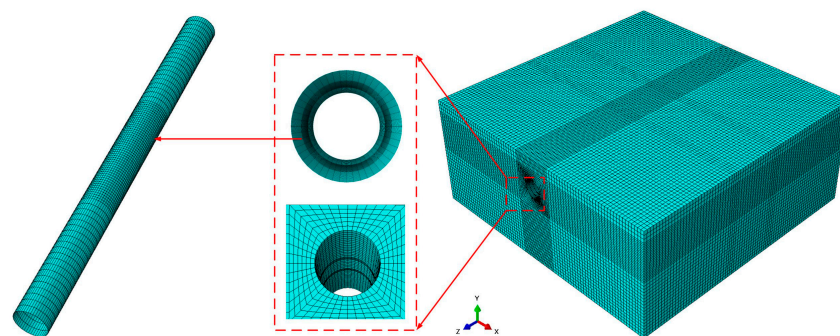


Figure 4. Pipe–soil mesh model.

Because the applied forces mainly acted on the portion of the model under wheel pressure, larger meshes were employed for the mesh divisions at the edges of the model. Consequently, the total number of elements in the modified model was 58,888. A comparison between the simulation results of the two distinct mesh configurations revealed that the data presented in Figure 5 differed by less than 1%.

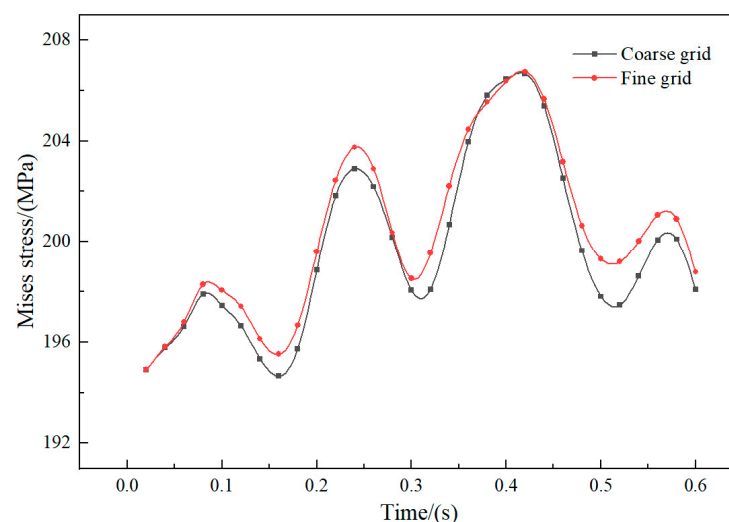


Figure 5. Maximum stress point duration of the pipeline stress curve.

4. Analysis of Results

By considering various influencing factors, such as heavy vehicle mass, pipeline parameters, soil properties, and operating pressure, an analysis of the mechanical behavior of the pipeline under typical conditions was conducted. A base case with a wall thickness of 18.5 mm, an outer diameter of 1016 mm, an internal pressure of 8 MPa, a burial depth of 1.5 m, a heavy vehicle mass of 50 t, and a vehicle speed of 54 km/h was analyzed.

This study investigated the effects of individual factors while simulating other influencing factors based on the base case. Through simulations, von Mises stress contour plots of the pipe–soil model were obtained. This facilitated the examination of the stress and strain patterns of the buried gas pipeline subjected to vehicular loads.

For the longitudinal mechanical analysis of the pipeline, the focus was on the top section of the pipe. The longitudinal displacement in the top section was regarded as the actual displacement of the pipeline.

The time point at which the pipeline underwent the maximum von Mises stress was 0.42 s (Figure 5). At this time, the center of mass of the vehicle was directly above the top of the pipeline. The stress contour plots for the pipeline before and after this time point are shown in Figure 6. During this specific time interval, the stress above the pipeline reached its peak value for the entire stage.

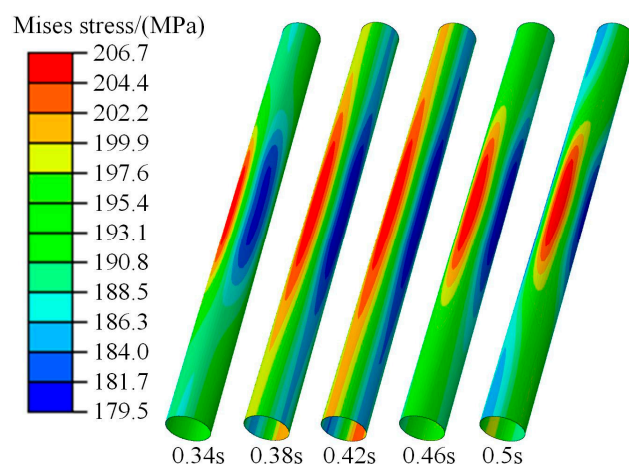


Figure 6. Time node–pipeline stress cloud (partial).

4.1. Pipe Diameter

Standard pipe diameters were selected for the analysis: 711, 813, 1016, and 1219 mm. The influence of heavy vehicle rolling loads on the pipeline was examined for these diameters. The diameter was regarded as a variable to analyze the mechanical response of the pipeline under heavy vehicle loads.

The axial von Mises stress distribution along the pipeline is shown in Figure 7. The maximum von Mises stress existed at the center of the pipeline, reaching 240 MPa. This point was above the middle axis of the wheels and not directly beneath the wheel–ground contact point. Therefore, if a vehicle passes over a pipeline without stopping, it will not damage the pipeline.

The diameter significantly influenced the von Mises stress in the pipeline (Figure 7). The axial von Mises stress along the pipeline axis significantly increased with increasing diameter. Under different diameter conditions, the vertical displacement of the pipeline exhibited similar scale characteristics, following a parabolic pattern. Typically, the mid-point of a pipeline experiences the highest displacement. As the diameter increased, the magnitude of the displacement decreased gradually.

By keeping other conditions constant, the maximum von Mises stress in the pipeline increased from 149.59 to 169.06 MPa when the outer diameter increased from 711 to 813 mm, indicating an increase of 13.02%. Similarly, as the outer diameter increased from 813 to 1016 mm, the maximum von Mises stress increased from 169.06 to 206.67 MPa, representing an increase of 22.25%. As the outer diameter increased from 1016 to 1219 mm, the maximum von Mises stress increased from 206.67 to 243.78 MPa, indicating an increase of 17.96%.

This analysis reveals that under identical vehicle conditions, a larger pipeline diameter results in a higher von Mises stress in the pipeline. However, the resulting deformation displacement in the pipeline decreased accordingly, implying a reduced influence of the vehicular load on the pipeline.

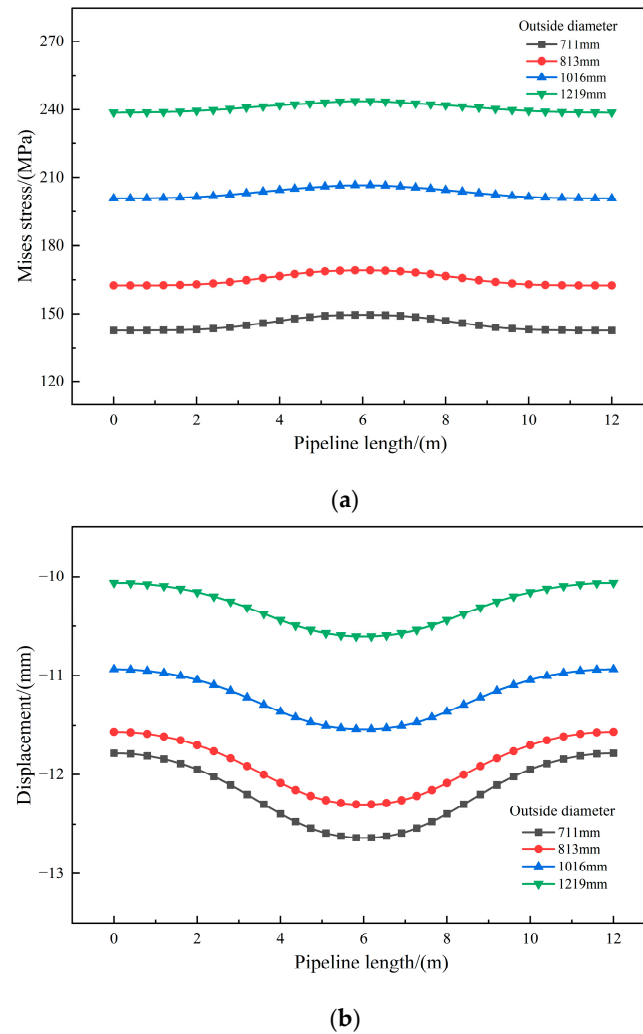


Figure 7. Stress/vertical displacement–pipe flow curve under different outer diameters. (a) Stress; (b) Vertical displacement.

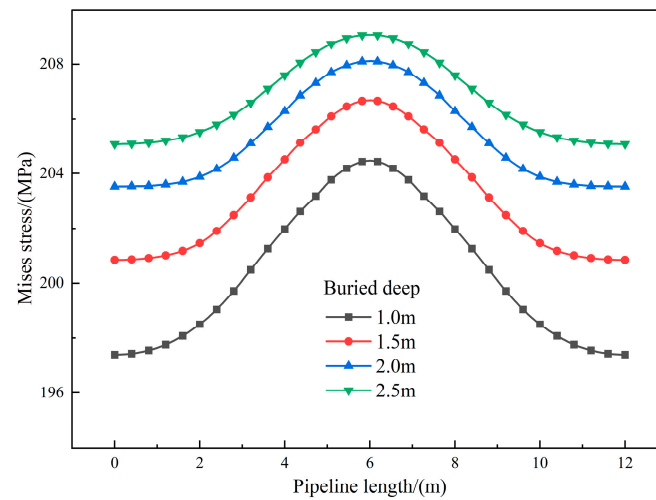
With an increase in the diameter, the overall stiffness of the pipeline increased. Under the same applied load, this increased stiffness implies an improved capacity to resist deformations. Consequently, the displacement of the pipeline decreased, consistent with the theoretical results. In practice, pipelines with large outer diameters are reinforced beneath, either by increasing the wall thickness of the pipeline or by incorporating reinforcing structures around the pipeline. These measures can enhance the load-bearing capacity of the pipeline and mitigate the impact of vehicles.

4.2. Pipe Depth

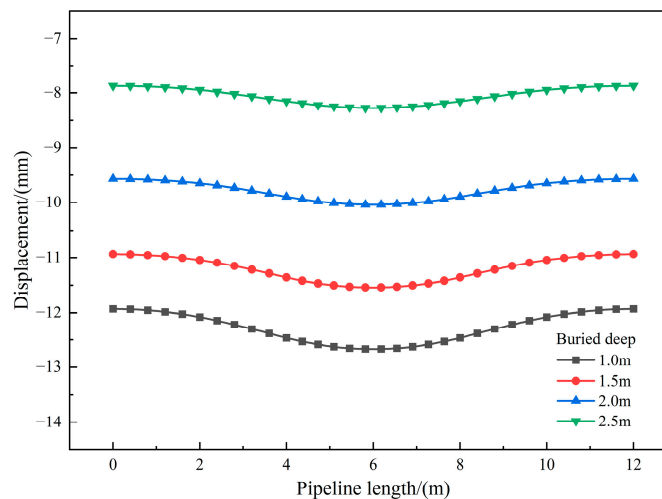
The burial depth of a pipeline is a critical factor that influences its mechanical deformation under loads. Different burial depths were selected as variables (1, 1.5, 2, and 2.5 m) to simulate the pipeline under various conditions.

Under different burial depths, the axial von Mises stress distribution along the pipeline showed a similar pattern (Figure 8). With increasing burial depth, the overburden load increased, whereas the stress generated by the vehicle load decreased. This combined effect leads to an overall decreasing trend in the von Mises stress of the pipeline. By keeping other conditions constant, the maximum von Mises stress in the pipeline increased from 203.45 to 206.67 MPa when the burial depth increased from 1.0 to 1.5 m, indicating an increase of 1.58%. Similarly, as the burial depth increased from 1.5 to 2.0 m, the maximum von Mises stress increased from 206.67 to 208.10 MPa, signifying an increase of 0.69%. With

an increase in the burial depth from 2.0 to 2.5 m, the maximum von Mises stress increased from 208.10 to 209.08 MPa, resulting in an increase of 0.47%.



(a)



(b)

Figure 8. Stress/vertical displacement–pipe flow curves under different burial depths. (a) Stress; (b) Vertical displacement.

The analysis revealed that the maximum axial von Mises stress in the pipeline occurred at its center because the pipeline ends were regarded as free constraints, leading to increased stress concentration at the center. As the burial depth increased, the von Mises stress at the top of the pipeline increased gradually. However, the stress gradient in the longitudinal direction of the pipeline diminished, indicating an enhanced interaction between the pipeline and soil with increasing burial depth, which resulted in a more uniform stress distribution. With an increase in the burial depth, the restraining effect of the soil on the pipeline increased. Compared with shallow-buried pipes, the force is more uniform.

As the burial depth increased, the pipeline stress induced by heavy vehicle rolling tended to stabilize with decreased fluctuations. A greater burial depth corresponded to a higher von Mises stress at the ends of the pipeline. This is attributed to the increased friction between the pipeline and soil, which effectively dispersed and transmitted the load induced by heavy vehicle traffic. The smaller the burial depth, the more obvious the influence of the pipeline by the ground traffic load; the von Mises stress difference

between the center and the two ends of the pipe section decreases, but the overall von Mises stress increases.

Practical burial depths for pipelines should be selected judiciously, considering the interaction between the soil and pipeline, to ensure stable stress distribution and structural integrity under heavy vehicle loads. Excessive burial depths can lead to increased installation costs, and overlying soil loads may result in excessive stress and the potential risk of structural failure.

4.3. Wheel Pressure Effects

Different vehicle weights resulted in varying tire pressures on the ground. For example, a 60 ton vehicle exerts a tire pressure of approximately 0.85 MPa on the ground. The impact of heavy vehicle loads can be indirectly reflected by altering the magnitude of the tire pressure. By keeping all other parameters constant, the influence of tire pressures of 0.7, 0.85, 1, and 1.15 MPa on the pipeline was investigated. The displacements and von Mises stresses in the pipeline for different vehicle weights are shown in Figure 9.

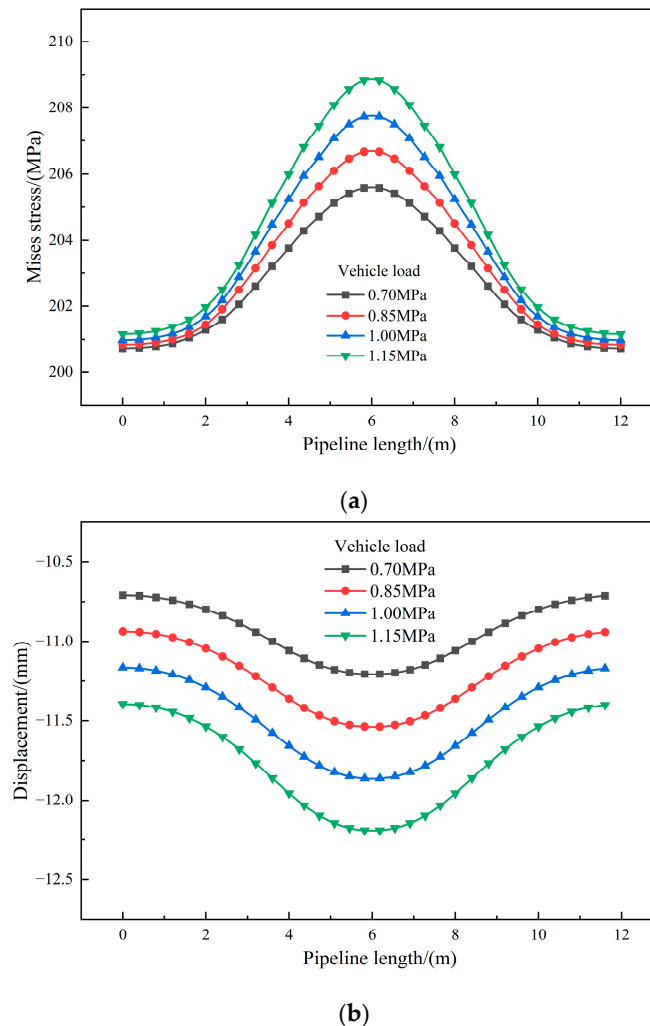


Figure 9. Stress/vertical displacement–pipe flow curve under different wheel pressures. (a) Stress; (b) Vertical displacement.

As the vehicle weight increased, the maximum stress in the pipeline increased, resulting in a more pronounced impact on the pipeline (Figure 9). However, the stresses at both ends of the pipeline remained almost unchanged, with the displacement mainly concentrated at the central point, where the pipeline was subjected to the most significant forces. By keeping other conditions constant, the maximum von Mises stress in the pipeline

increased from 205.42 to 206.47 MPa, indicating an increase of approximately 0.51%. Similarly, when the tire pressure increased from 0.85 to 1.00 MPa, the maximum von Mises stress increased from 206.47 to 207.49 MPa, representing an increase of approximately 0.49%. Furthermore, as the tire pressure increased from 1.00 to 1.15 MPa, the maximum von Mises stress in the pipeline increased from 207.49 to 208.57 MPa, showing an increase of approximately 0.52%. For every incremental rise (0.15 MPa) in the load per tire, the maximum von Mises stress in the pipeline increased by approximately 0.5%.

When the magnitude of the vehicle load changed, the stress on the pipeline underwent corresponding variations, mainly exhibited as changes in the peak stress values rather than alterations in the waveform. In practical applications, casings or protective measures are introduced to mitigate the risk of damage caused by rolling loads.

4.4. Internal Pressure in Pipelines

By keeping other parameters constant, the internal pressure of the conveyed medium was varied, with values of 4, 6, 8, and 10 MPa.

Similar to the results obtained for variations in the pipe diameter under different internal pressures, the pipeline stress increased with increasing internal pressure (Figure 10). The von Mises stress induced by vehicle rolling resulted in elevated stress levels within the pipeline as the vehicle approached it.

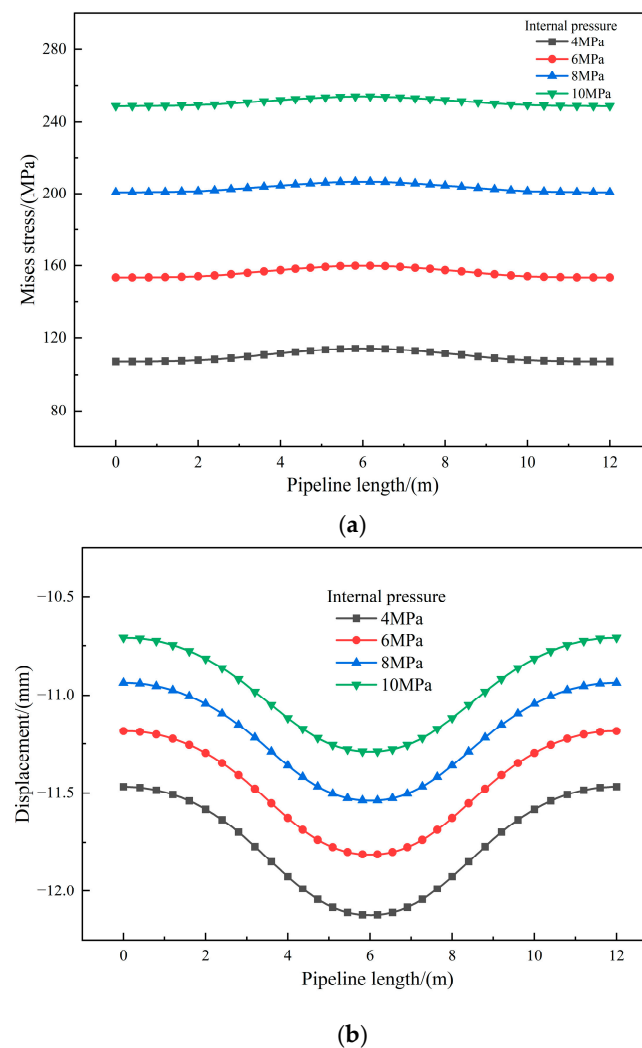


Figure 10. Stress/vertical displacement–pipe flow curve under different internal pressures. (a) Stress; (b) Vertical displacement.

With other conditions remaining constant, the maximum von Mises stress in the pipeline increased from 114.08 to 159.94 MPa when the internal pressure of the pipeline increased from 4 to 6 MPa, which is an increase of approximately 40.20%. Similarly, as the internal pressure increased from 6 to 8 MPa, the maximum von Mises stress in the pipeline increased from 159.94 to 206.67 MPa, showing an increase of approximately 29.22%. Finally, as the internal pressure increased from 8 to 10 MPa, the maximum von Mises stress in the pipeline increased from 206.67 to 253.95 MPa, an increase of approximately 22.88%.

Based on the analysis, under identical conditions, the maximum von Mises stress induced by vehicle rolling decreased as the internal pressure of the pipeline increased. However, this decrease was significantly less than the increase in the Mises stress generated by the internal pressure of the pipeline. Pipelines with high internal pressures exhibit significant resistance to the effects of vehicle rolling loads. Across the different internal pressure scenarios, the distribution pattern of the maximum stress induced by heavy vehicle rolling remained consistent along the length of the pipeline. The effect of internal pressure on the stress distribution pattern within the pipeline was minimal.

5. Conclusions

In this study, a finite element model of buried pipelines under vehicle rolling loads was established, considering the comprehensive effects of pipe–soil interactions and reflecting the mechanical response characteristics of pipelines under heavy loads. The model precisely accounted for the interaction between the pipeline and the surrounding soil and quantitatively described essential parameters, such as stress, displacement, and deformation, under vehicle rolling loads. Mechanical analyses were conducted based on four aspects: pipeline outer diameter, pipeline burial depth, internal pressure, and traffic load. The following conclusions were drawn:

Heavy vehicles passing over the pipeline caused the deformation of the buried pipeline. As vehicles traversed buried gas pipelines, the von Mises stress experienced by the pipeline increased with increasing diameter, internal pressure, and vehicle self-weight but decreased with increasing burial depth.

This study revealed that the primary loads on the pipeline when vehicles pass over it are the internal pressure and overburden loads. The additional stress imposed by vehicle loads on the X80 gas pipeline did not exceed 10 MPa. Under normal conditions, the X80 buried gas pipeline underwent deformation when subjected to vehicle rolling, with the maximum deformation occurring along the central axis of the vehicle. Altering various parameters yielded a maximum deformation of 13 mm. The buried X80 gas pipeline was not prone to damage from brief heavy vehicle rolling loads. In practical scenarios, considering the long-term operation of a pipeline, reinforcement measures can be provided beneath the pipeline to enhance its load-bearing capacity. Alternatively, buffer zones around the pipeline, such as flexible materials or filling with sand, can help alleviate the pressure from vehicle loads and reduce the risk of pipeline deformation owing to rolling. For large vehicles intermittently applying heavy rolling loads to pipelines in frequently traveled road sections, future research should investigate the effect of dynamic road vehicle loads on pipeline fatigue failure and its applicability.

Author Contributions: Conceptualization, J.Z. and X.G.; methodology, Y.Z. (Yutong Zhou); software, J.Z.; validation, Y.W.; formal analysis, H.Z.; investigation, J.Z.; resources, X.G.; data curation, J.Z.; writing—original draft preparation, J.Z.; writing—review and editing, J.Z. and X.G.; visualization, X.G.; supervision, X.G.; project administration, X.G.; funding acquisition, Y.Z. (Yuan Zhang). All authors have read and agreed to the published version of the manuscript.

Funding: This research received no external funding.

Data Availability Statement: Not applicable.

Conflicts of Interest: The authors declare no conflict of interest.

References

1. Zhang, D.; Zhang, H.; Zhou, Y.; Shi, N.; Jiang, J.; Shi, N.; Wu, Z.; Liu, X. Mechanical response of X65 pipeline under rolling compaction of heavy trucks and the influencing factors. *Oil Gas Storage Transp.* **2022**, *41*, 177–184.
2. Phillips, R.; Nobahar, A.; Zhou, J. Combined axial and lateral pipe–soil interaction relationships. In Proceedings of the International Pipeline Conference, Calgary, AB, Canada, 4–8 October 2004; Volume 41766, pp. 299–303.
3. Yimsiri, S.; Soga, K.; Yoshizaki, K.; Dasari, G.R.; O'Rourke, T.D. Lateral and upward Soil–Pipeline interactions in sand for deep embedment conditions. *J. Geotech. Geoenviron. Eng.* **2004**, *130*, 830–842. [[CrossRef](#)]
4. Alzabeebee, S.; Chapman, D.N.; Faramarzi, A. A comparative study of the response of buried pipes under static and moving loads. *Transp. Geotech.* **2018**, *15*, 39–46. [[CrossRef](#)]
5. Mitra, A.C.; Fernandes, E.; Nawpute, K.; Sheth, S.; Kadam, V.; Chikhale, S.J. Development and Validation of a Simulation Model of Automotive Suspension System using MSC-ADAMS. *Mater. Today Proc.* **2018**, *5*, 4327–4334. [[CrossRef](#)]
6. Li, B.; Fang, H.; Yang, K.; Zhang, X.; Du, X.; Wang, N.; Guo, X. Impact of erosion voids and internal corrosion on concrete pipes under traffic loads. *Tunn. Undergr. Space Technol.* **2022**, *130*, 104761. [[CrossRef](#)]
7. Rakitin, B.; Xu, M. Centrifuge modeling of large-diameter underground pipes subjected to heavy traffic loads. *Can. Geotech. J.* **2014**, *51*, 353–368. [[CrossRef](#)]
8. Zamanian, S.; Shafieezadeh, A. Temporal global sensitivity analysis of concrete sewer pipes under compounding corrosion and heavy traffic loads. *Struct. Infrastruct. Eng.* **2023**, *19*, 1108–1121. [[CrossRef](#)]
9. Robert, D.J.; Chan, D.; Rajeev, P.; Kodikara, J. Effects of operational loads on buried water pipes using field tests. *Tunn. Undergr. Space Technol.* **2022**, *124*, 104463. [[CrossRef](#)]
10. Wu, X. Study on the Mechanical Analysis Model of Pipelines in Soft Ground Under Traffic Loads. Ph.D. Thesis, Civil Engineering of Zhejiang University, Hangzhou, China, 2004.
11. Wang, Z. Study on Mechanical Behaviors of Buried Pipelines Under Traffic Loads. Ph.D. Thesis, Zhejiang University, Hangzhou, China, 2006.
12. Liao, N.; Huang, K.; Wu, J.; Chen, L.; Lyu, Y. Analysis on mechanical properties of gas pipeline crossing highway based on ABAQUS. *J. Saf. Sci. Technol.* **2017**, *13*, 61–67.
13. Jiang, W.; Miao, L.; Wang, Y.; Gan, Y.; Jiao, S.; Zhang, H.; Xu, T. Study on Dynamic Response of Buried Pipeline Rolled by Heavy Vehicle Based on Co-simulation by ADAMS and ABAQUS. In *Journal of Physics: Conference Series*; IOP Publishing: Bristol, UK, 2022; Volume 2185, p. 012018.
14. Zhu, L.; Wu, G.; Li, L.; Luo, J.; Tian, Y.; Xu, C.; Lin, R. Strain evolution characteristics of X80 line pipes with plain dents. *Nat. Gas Ind.* **2019**, *39*, 113–119. [[CrossRef](#)]
15. Vazouras, P.; Karamanos, S.A.; Da Koulas, P. Finite element analysis of buried steel pipelines under strike-slip fault displacements. *Soil Dyn. Earthq. Eng.* **2010**, *30*, 1361–1376. [[CrossRef](#)]
16. Zhang, J.; Liang, Z.; Han, C.J. Buckling behavior analysis of buried gas pipeline under strike-slip fault displacement. *J. Nat. Gas Sci. Eng.* **2014**, *21*, 921–928. [[CrossRef](#)]
17. Shirokov, V.S. Soil and Traffic Loads on Underground Pipelines. *Soil Mech. Found. Eng.* **2018**, *55*, 115–119. [[CrossRef](#)]
18. Zhang, P.; Yao, Z. Study on mechanical behavior of buried PE pipeline with defect under traffic load. *J. Saf. Sci. Technol.* **2020**, *16*, 25–31.
19. Guo, T.; Pel, Z.; Huang, X. FEM Simulation and Safety Evaluation of Dented Oil-Gas Pipeline. *J. Xi'an Shiyou Univ. (Nat. Sci. Ed.)* **2022**, *37*, 99–104+122.
20. He, P. The Generalized Modal Method in Finite Element Design with Its Application. Ph.D. Thesis, Northwestern Polytechnical University, Xi'an, China, 2017.
21. Zhang, D.; Liu, X.; Yang, Y.; Shi, N.; Jiang, J.; Chen, P.; Zhang, H. Field experiment and numerical investigation on the mechanical response of buried pipeline under traffic load. *Eng. Fail. Anal.* **2022**, *142*, 106734. [[CrossRef](#)]

Disclaimer/Publisher's Note: The statements, opinions and data contained in all publications are solely those of the individual author(s) and contributor(s) and not of MDPI and/or the editor(s). MDPI and/or the editor(s) disclaim responsibility for any injury to people or property resulting from any ideas, methods, instructions or products referred to in the content.